Original Article

Oxymatrine attenuates arsenic-induced endoplasmic reticulum stress and calcium dyshomeostasis in hepatic stellate cells

Huiqun Wang[1,2,3], Bing Han[1,2], Nanlan Wang[1,3], Yang Lu[3], Ting Gao[4], Zihan Qu[3], Hongmei Yang[3], Qin Yang[1,3]

[1]Guizhou Provincial Key Laboratory of Pathogenesis & Drug Research on Common Chronic Diseases, [2]Department of Pathophysiology, [3]Key Laboratory of Environmental Pollution Monitoring and Disease Control, Ministry of Education, Guizhou Medical University, Guiyang, China; [4]Department of Pathology, the Affiliated Hospital of Guizhou Medical University, Guiyang, China

Contributions: (I) Conception and design: H Wang, Q Yang; (II) Administrative support: Q Yang; (III) Provision of study materials or patients: H Wang, B Han, N Wang, Y Lu; (IV) Collection and assembly of data: H Wang; (V) Data analysis and interpretation: H Wang; (VI) Manuscript writing: All authors; (VII) Final approval of manuscript: All authors.

Correspondence to: Qin Yang. Guizhou Provincial Key Laboratory of Pathogenesis & Drug Research on Common Chronic Diseases, Guizhou Medical University, Guiyang, China. Email: Qinyang_YQ@163.com.

Background: Oxymatrine is the main bioactive component of Sophora flavescens. It exhibits various biological activities and has been used in various liver diseases, including hepatic fibrosis (HF). Hepatic stellate cells (HSCs) are the primary cell type involved during HF progression. Oxymatrine treatment could suppress the proliferation of HSCs and degrade the extracellular cell matrix (ECM), presumed to be associated with HF. However, the mechanism is still unknown.

Methods: $NaAsO_2$ induces HF in LX2 cells. Oxymatrine was used to treat $NaAsO_2$- induced LX2 cells. Then, the LX2 cell proliferation, apoptosis, ECM secretion protein, oxidative stress index, and intracellular calcium concentration were respectively measured. Furthermore, after knocking down GRP78 [endoplasmic reticulum (ER) chaperone BiP] or overexpressing of SERCA2 (ATPase sarcoplasmic/ER Ca^{2+} transporting 2) in $NaAsO_2$-induced LX2 cells, we detected the changes in ER stress and calcium homeostasis in LX2 cells.

Results: $NaAsO_2$ exposure promoted apoptosis, increased ECM secretion, produced ER stress, and disrupted calcium homeostasis, which could be attenuated by oxymatrine treatment. Furthermore, knockdown of GRP78 to alleviate ER stress, or overexpression of SERCA2 to restore intracellular calcium homeostasis can inhibit the $NaAsO_2$ effect.

Conclusions: Oxymatrine treatment could improve calcium homeostasis and attenuate ER stress to reverse $NaAsO_2$-induced HSC activation and ECM secretion, which are the significant phenotypes of HF. The ER stress and calcium homeostasis may be the therapeutic targets for HF.

Keywords: Oxymatrine; endoplasmic reticulum stress (ER stress); calcium homeostasis; GRP78; SERCA2

Submitted Jul 16, 2020. Accepted for publication Sep 04, 2020. This article was updated on September 13, 2024.
The original version is available at: http://dx.doi.org/10.21037/atm-20-5881
doi: 10.21037/atm-20-5881

Introduction

Hepatic fibrosis (HF) is a severe liver disease characterized by abnormal hyperplasia and the accumulation of extracellular cell matrix (ECM) (1-4). Chronic injury, including following alcohol abuse, chronic hepatic virus infection, exposure to toxic substances, and various diseases, may induce repetitive tissue damage and reduce the regenerative capacity of the liver and promote the necrosis or apoptosis of parenchymal cells, which are replaced by ECM (5). With disease progression, HF would be worse for patients with liver cancer, eventually leading to hepatic failure and mortality (1). However, if treated at an early stage, to eliminate pathogenic factors, HF could be reversed (2). Arsenic is a group 1 carcinogenic substance and is widely distributed in the earth (6). It has been reported

that drinking water in several countries and regions contains an excessive amount of arsenic and has been a public health risk (6). Chronic exposure to inorganic arsenic can induce several cancer types, including in the kidney, skin, and liver. The liver is one of the primary target organs for arsenic toxicity (7). Furthermore, earlier studies have proved that chronic arsenic exposure can induce HF in mice and rat models (8,9). However, the mechanism is still unknown.

Several traditional Chinese medicines have been used to treat diseases. Oxymatrine, the main bioactive component of *Sophora flavescens* (10,11), exhibits various biological activities, including acting as an anti-inflammatory, anti-cancer, anti-fibrosis, and antiviral agent, inhibiting the hepatitis B virus (12,13). Oxymatrine has been used for the treatment of various liver diseases, including viral hepatitis and chronic liver disease, for an extended period in China (13,14). Moreover, oxymatrine treatment could suppress the proliferation of hepatic stellate cells (HSCs) and degrade the ECM, presumed to be associated with HF (15,16). However, the mechanism is not well understood.

With these studies above, the present study used $NaAsO_2$ and oxymatrine to treat the LX2 cell line to study the underlying mechanism of $NaAsO_2$ induced HSC activation, apoptosis, and ECM secretion and the effects of oxymatrine treatment. Furthermore, the role of ER stress was investigated. We present the following article in accordance with the MDAR reporting checklist (available at http://dx.doi.org/10.21037/atm-20-5881).

Methods

Cell culture

The human LX2 cell line was bought from the Type Culture Collection of the Chinese Academy of Sciences. Cells were cultured in DMEM (Gibco; Thermo Fisher Scientific, Inc., USA), supplemented with 10% FBS (Gibco; Thermo Fisher Scientific, Inc., USA) and 1% penicillin-streptomycin (Gibco; Thermo Fisher Scientific, Inc., USA). These cells are supported in a humidified incubator with 5% CO_2 at 37 ℃.

Cell Counting Kit-8 (CCK-8) assay

Cell proliferation was determined using the CCK-8 assay, as previously described (17). Briefly, LX2 cells were digested using 0.25% trypsin and seeded in 96-well plates at a density of 3.0×10^4 cells/mL. CCK-8 (Dojindo Molecular Technologies, Inc., Japan) was used to measure LX2 cell proliferation, according to the manufacturers' protocol. The optical density was measured at a wavelength of 450 nm. Triplicate wells were set up for each sample, and the experiment was repeated three times.

ELISA

The levels of ECM secretion, including hyaluronic acid (HA; R&D Systems, Inc., USA), collagen type IV (COL-IV; CUSABIO), and rat/human TGF-β1 (cat. no. ab100647; Abcam), were determined by ELISA, according to the manufacturers' protocols.

Flow cytometry assay

Apoptosis rates were determined using flow cytometry and Annexin V-FITC and propidium iodide (BD Biosciences) double staining, as previously described (18). Briefly, LX2 cells were washed twice with cold PBS and resuspended at a concentration of 1×10^6 cells/mL in a 1× binding buffer. In total, 100 μL of cell suspension was incubated with 5 μL Annexin V-FITC and 5 μL of PI for 15 min at 25 ℃. After 400 μL of 1× binding buffer was added to the cell suspension, flow cytometry analyzed apoptosis using Becton Dickinson FACS Calibur flow cytometer (BD, USA).

Western blot analysis

Samples were lysed in a cold RIPA buffer (150 mM NaCl, 1% Triton X-100, 0.5% sodium deoxycholate, 0.1% SDS and 50 mM Tris-HCl, pH 8) supplemented with 1% protease inhibitor (Thermo Fisher Scientific, Inc., USA). The protein concentration was determined using BCA. Protein samples (60 μg) were separated using 10% SDS-PAGE and transferred to PVDF membranes (Millipore) according to the standard protocol. GAPDH and β-actin were used as an endogenous control for protein loading. The following primary antibodies were: α-smooth muscle actin (α-SMA; 1:800, cat. no. 48938S; Cell Signaling Technologies, Inc., USA), calpain 2 (1:1,000, cat. no. 2539S; Cell Signaling Technologies, Inc.), DNA damage-inducible transcript 3 protein (CHOP; 1:800, cat. no. 2895S; Cell Signaling Technologies, Inc.), endoplasmic reticulum (ER) chaperone BiP (GRP78; 1:1,000, cat. no. 3183S; Cell Signaling Technologies, Inc.), ATPase sarcoplasmic/ER Ca^{2+} transporting 2 (SERCA2; 1:800, cat. no. 4388S; Cell Signaling Technologies, Inc., USA), cleaved caspase 12 (1:700 cat. no. 2202; Cell Signaling Technologies,

Table 1 Sequences of primers used for reverse transcription-quantitative PCR

Genes	Forward primer (5'-3')	Reverse primer (5'-3')
RYR1	CTCCGCCTCTTTCATGGACAT	CTGCCCGGTAGTGACATGC
CAPN2	GAAGCGTCCCACGGAACTG	GTGCAGGAGGGTGTCGTTG
GRP78	CATCACGCCGTCCTATGTCG	CGTCAAAGACCGTGTTCTCG
CHOP	GAACGGCTCAAGCAGGAAATC	TTCACCATTCGGTCAATCAGAG
SERCA2	AAACCACGGAGGAATGTTTGG	AGCTCATTGAGGCCGTATTTC
GAPDH	AGAAGGCTGGGGCTCATTTG	AGGGGCCATCCACAGTCTTC

Inc.), GAPDH (1:5,000 cat. no. 5174; Cell Signaling Technologies, Inc.) and β-actin (1:5,000, cat. no. 4970; Cell Signaling Technologies, Inc.). After incubating with the secondary antibody (goat anti-rabbit and anti-mouse IgG, HRP 1:20,000, ZSGB-Bio, China) for one hour at room temperature. Western Lighting ECL visualized protein bands using the VersaDoc imaging system (Biorad, Hercules, CA, USA) and quantified using QuantityOne software (Biorad).

Oxidative stress-related index detection

Malondialdehyde (MDA) and total superoxide dismutase (T-SOD) activities were detected using malondialdehyde MDA and T-SOD kits (Nanjing Jiancheng Bioengineering Institute) and were performed according to the manufacturer's instructions.

Reverse transcription-quantitative (RT-q) PCR

Cellular total RNA was isolated using TRIzol reagent (Takara Bio, Inc., Japan), according to the manufacturer's instructions. Complementary (c) DNA and QPCR were performed according to the manufacturer's instructions. Primers for the qPCR were designed using Primer 5.0 (*Table 1*). GAPDH was used as an endogenous control for normalization. Data were analyzed using the $2^{-\Delta\Delta Ct}$ method.

Measurement of calcium concentration

The intracellular calcium concentration in LX2 cells was determined using flow cytometry, as previously described (19). Briefly, LX2 cells were cultured in a 6-well plate and grown until a confluence of 70%. A cell-permeable 5 μM calcium-binding dye and probenecid (Thermo Fisher Scientific, Inc.) were added to the culture medium and incubated at 37 ℃ for 30 min. LX2 cells were harvested, pelleted (800 ×g, 4 ℃, 5 min), and suspended in a Ca^{2+} free Krebs-Ringer buffer, and the calcium concentration was determined using flow cytometry.

GRP78 and SERCA2 knockdown and overexpression

Short hairpin (sh)RNA is used to knockdown endogenous GRP78 and SERCA2 expression. IGEbio synthesized control and shRNA. The sequences of human GRP78-shRNA/control and SERCA2-shRNA/control are listed in *Table 2*. Human GRP78, SERCA2 cDNA (Gene ID. 3309 and 488, respectively), control and shRNA were synthesized and cloned into the pCDH-CMV-MCS-EF1-Puro vector (7,384 bp, Aiji biotechnology co., Guangzhou, LTD) to overexpressing/knockdown GRP78 and SERCA2 in LX2 cells. The empty vector was used as the control of GRP78/SERCA2 overexpression, while scram sequences were used as the control of shRNA. The transfections were conducted using Lipofectamine 3000 (Gibco; Thermo Fisher Scientific, Inc., USA), according to the manufacture's protocol. The GRP78 and SERCA2 knockdown and overexpression were confirmed using western blotting and RT-qPCR compared to negative controls.

Statistical analysis

All data are expressed as the mean ± SD. Statistical comparisons were performed using SPSS 19.0 software (IBM Corp). Unpaired two-sample *t*-tests were performed for comparisons between the two groups. Three comparisons were determined using one-way ANOVA followed by the least significant difference test, while four or more comparisons using one-way ANOVA followed by Tukey. $P<0.05$ was considered to indicate a statistically significant difference.

Table 2 GRP78 and SERCA2 shRNA sequences

Genes	shRNA Sequence
GRP78-Control	5'-TGCGCCTTACATACTGGTTTGCTAAAAA TCCACTACTGAGAATCTACGAATGTTTGTG GTTG-3'
GRP78-shRNA1	5'-CCGGGTTCAACGACCTTCGCTTCGTC TCGAGACGAAGCGAAGGTCGTTGAACTT TTTGAATT-3'
GRP78-shRNA2	5'-CCGGGAAATCGAAAGGATGGTTAATCT CGAGATTAACCATCCTTTCGATTTCTTTTT GAATT-3'
GRP78-shRNA3	5'-CCGGAGATTCAGCAACTGGTTAAAGCT CGAGCTTTAACCAGTTGCTGAATCTTTTTT GAATT-3'
SERCA2-Control	5'-AAGGGCCTAAATTGTCTAGTCGTGTGT CTCTGTTCCACGTACGTAGATCCGACCCA AGTGTG -3'
SERCA2-shRNA1	5'-CCGGCCCTTGGTTGTACTTCTGTTACT CGAGTAACAGAAGTACAACCAAGGGTTTT TGAATT-3'
SERCA2-shRNA2	5'-CCGGCCATCAAATCTACCACACTAACT CGAGTTAGTGTGGTAGATTTGATGGTTTTT GAATT-3'
SERCA2-shRNA3	5'-CCGGGGCTAGCAGCATGCGGTATTTCT CGAGAAATACCGCATGCTGCTAGCCTTTT TGAATT-3'

shRNA, short hairpin RNA.

Results

Oxymatrine suppresses $NaAsO_2$-induced LX2 activation and ECM secretion

Earlier studies have shown that HF is associated with the activation of HSCs (5,10). Inhibition of HSCs may reduce ECM production and promote ECM degradation, an effective strategy to prevent and treat HF. The LX2 cell line, an immortalized human HSC cell line, has been widely used for liver-related research. In the present study, LX2 was selected as an *in vitro* model to investigate the underlying mechanism of $NaAsO_2$-induced HSC apoptosis, activation and ECM secretion, and the effects of oxymatrine. First, it was determined whether $NaAsO_2$ treatment could promote proliferation in LX2 cells in a dose- and time-dependent manner. The results from the CCK-8 assay showed that 0.5 and 1 μM $NaAsO_2$ promoted LX2 proliferation in a time-dependent manner (*Figure 1A*). Oxymatrine was used to treat LX2 cells following this, and it was found that oxymatrine could inhibit 1 μM $NaAsO_2$ induced proliferation (*Figure 1B*). Therefore, this concentration was selected for later experiments. Flow cytometry analysis was employed to determine the apoptosis in the LX2 cell line and found $NaAsO_2$ treatment promoted apoptosis in the LX2 cell and which was suppressed by treatment with oxymatrine (*Figure 1C*). ELISA results showed that NaAsO2 exposure enhanced ECM secretion and that this was suppressed by treatment withoxymatrine (*Figure 1D,E*). As we know, the expression of α-SMA was one of the indicators for HSC activation. Compared with the control, $NaAsO_2$ increased the level of α-SMA, and this was inhibited by treatment with oxymatrine (*Figure 1F*). The changes in α-SMA expression indicated $NaAsO_2$ exposure could increase active HSCs and that OM suppressed this. With the HSC activation, ECM secretion would be increased, and it is the vital phenotype for HF. Then, SOD and MDA levels were detected to evaluate the level of oxidative stress. It was found $NaAsO_2$ promoted oxidative stress and that this was reserved by treatment with oxymatrine (*Figure 1G,H*).

Oxymatrine suppresses $NaAsO_2$-induced ER stress

ER's stress is one of the major causes of HSC activation (16); we hypothesize oxymatrine suppressed $NaAsO_2$ by attenuating ER stress. The Q-PCR results of CHOP, GRP78, SERCA2, CAPN2, and RyR1 indicated that treatment could attenuate $NaAsO_2$-induced ER stress with oxymatrine (*Figure 2A,B*). Calpain2, CHOP, GRP78, and SERCA2 protein levels were also determined to evaluate the level of ER stress. The western blot analysis also showed $NaAsO_2$ induced ER stress and that this was attenuated by treatment with oxymatrine (*Figure 2C*). Due to the association between ER stress and calcium homeostasis, cellular calcium concentration was determined. After $NaAsO_2$ treatment, the cellular calcium level was increased, and this was blocked by treatment with oxymatrine (*Figure 2D*). From these data, it was concluded that ER stress and cellular calcium homeostasis are associated with $NaAsO_2$ and oxymatrine treatment in LX2 cells.

Knockdown of GRP78 attenuated $NaAsO_2$-induced LX2 activation and ECM secretion

To further determine the role of ER stress in $NaAsO_2$-induced HSC activation and the mechanism of oxymatrine treatment, we altered the GRP78 expression to regulate

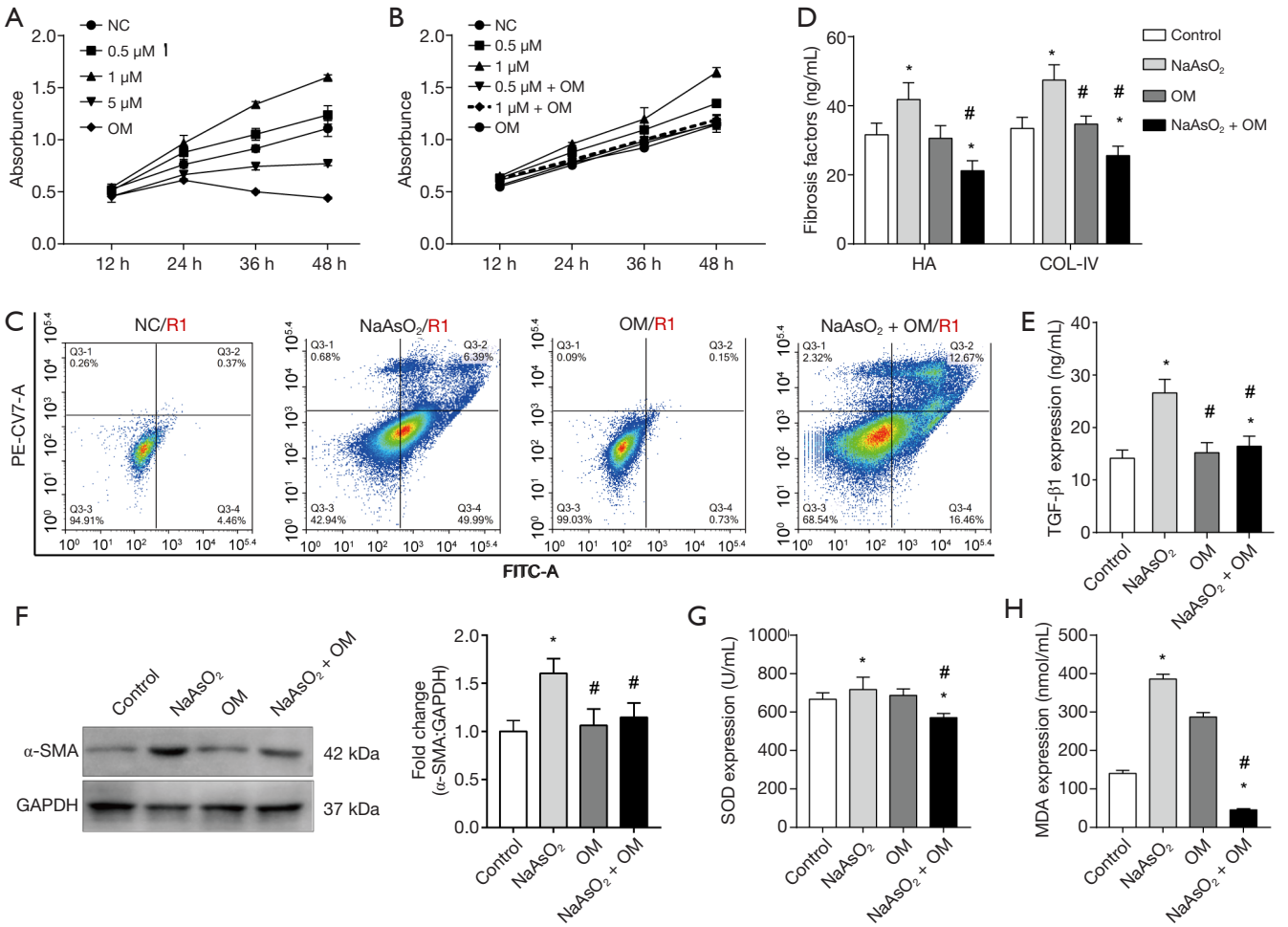

Figure 1 Oxymatrine suppresses $NaAsO_2$-induced LX2 activation and ECM secretion. (A,B) LX2 cell proliferation determined with CCK-8 assay after exposure to $NaAsO_2$ and OM in a dose- and time-dependent manner. (C) Flow cytometry analysis of LX2 cells after exposure to $NaAsO_2$ and OM. (D,E) HA, COL-IV, and TGF-β1 expression was determined using ELISA. (F) Western blotting and statistical analysis of α-SMA protein level. (G,H) SOD and MDA expression after $NaAsO_2$ and OM exposure. Data are presented as the mean ± SD, n=6, *, $P<0.05$ *vs.* control; #, $P<0.05$ *vs.* $NaAsO_2$ group. ECM, extracellular cell matrix; CCK-8, Cell Counting Kit-8; OM, oxymatrine; α-SMA, α-smooth muscle actin; HA, hyaluronic acid; COL-IV, collagen type IV; SOD, superoxide dismutase; MDA, malondialdehyde.

ER stress in the later experiments. The protein levels of GRP78 were examined, and it was found overexpression enhanced GRP78 expression, while the shRNA reduced GRP78 expression (*Figure 3A*). After it, the level of LX2 apoptosis was determined using flow cytometry and the protein level of cleaved caspase 12. Our analysis showed that the knockdown of GRP78 inhibited $NaAsO_2$-induced apoptosis (*Figure 3B,C*). The protein level of α-SMA was examined to assess whether alteration of GRP78 expression prevented $NaAsO_2$-induced LX2 cell activation. Compared with $NaAsO_2$ treatment, GRP78 knockdown significantly reduced α-SMA expression (*Figure 3C*). The protein level of CHOP, associated with the ER stress, was increased by $NaAsO_2$ treatment and rescued by GRP78 shRNA (*Figure 3C*). Subsequently, ECM secretion was measured to investigate whether the knockdown of GRP78 blocked the $NaAsO_2$-induced ECM secretion. Compared with $NaAsO_2$ treatment, GRP78 knockdown reduced TGF-β1, HA, and COL-IV expression (*Figure 3D,E*). So, we could conclude attenuation of ER stress could reverse $NaAsO_2$ induced LX2 activation and ECM secretion, which are the significant drivers of HF.

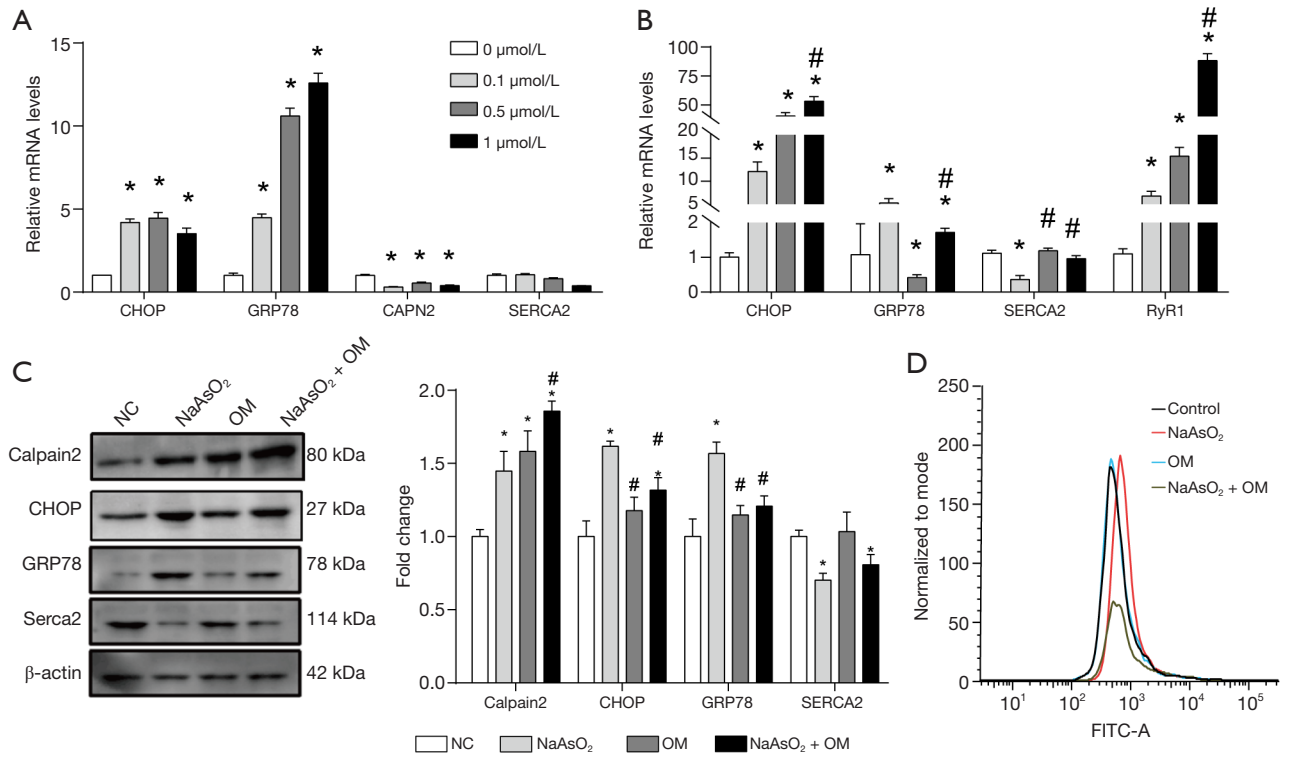

Figure 2 Oxymatrine suppresses $NaAsO_2$-induced endoplasmic reticulum stress. (A, B) The relative mRNA of CHOP, GRP78, SERCA2, RyR1 expression after exposure to $NaAsO_2$ and OM in LX2 cells. (C) Western blotting and statistical analysis of Calpain2, CHOP, GRP78, and SERCA2. (D) Calcium concentration in LX2 cells after exposure to $NaAsO_2$ and OM. Data are presented as the mean ± SD, n=6. *, P<0.05 *vs.* control; #, P<0.05 *vs.* $NaAsO_2$ group. OM, oxymatrine; CHOP, DNA damage-inducible transcript 3 protein; RyR1, ryanodine receptor.

Overexpression of SERCA2 recovers $NaAsO_2$-induced LX2 activation and ECM secretion

Given that $NaAsO_2$ and oxymatrine treatment could affect cellular calcium concentration, the endogenous levels of SERCA2 were also altered to regulate calcium homeostasis in the later experiments. The protein levels of SERCA2 were examined, and it was found overexpression enhanced SERCA2 expression, while the shRNA reduced SERCA2 expression (*Figure 4A*). The mRNA levels of CHOP and GRP78 showed that alteration of serca2 could affect ER stress in LX2 cells. Both the overexpression and knockdown of SERCA2 increased CHOP expression. The expression of GRP78 was inhibited by SERCA2 overexpressed and increased by SERCA2 knockdown (*Figure 4B*), indicating that overexpression of SERCA2 could cause attenuation of $NaAsO_2$ induced ER stress. The protein levels of cleaved caspase 12 were determined to evaluate the level of LX2 apoptosis. $NaAsO_2$ treatment increased the cleaved-caspase12 and could be inhibited by SERCA2 overexpression (*Figure 4C*). Then, the protein level of α-SMA was determined to evaluate LX2 activation. The western blot analysis of α-SMA showed that knockdown SERCA2 could aggravate $NaAsO_2$-induced LX2 cell activation (*Figure 4D*). Also, we found that SERCA2 overexpression reduced the $NaAsO_2$-increased ECM secretion, including TGF-β1, HA, and COL-IV (*Figure 4E,F*). Flow cytometry analysis was employed to investigate the effect of $NaAsO_2$ and oxymatrine on the intracellular calcium concentration and the role it played in SERCA2. Compared with the control, SERCA2 knockdown increased calcium concentration. It was found that SERCA2 overexpression could recover the $NaAsO_2$ induced cellular calcium dyshomeostasis in LX2 cells (*Figure 4G*). These data showed that overexpression of SERCA2 to restore calcium homeostasis could inhibit $NaAsO_2$ induced ER stress, LX2 activation, and ECM secretion.

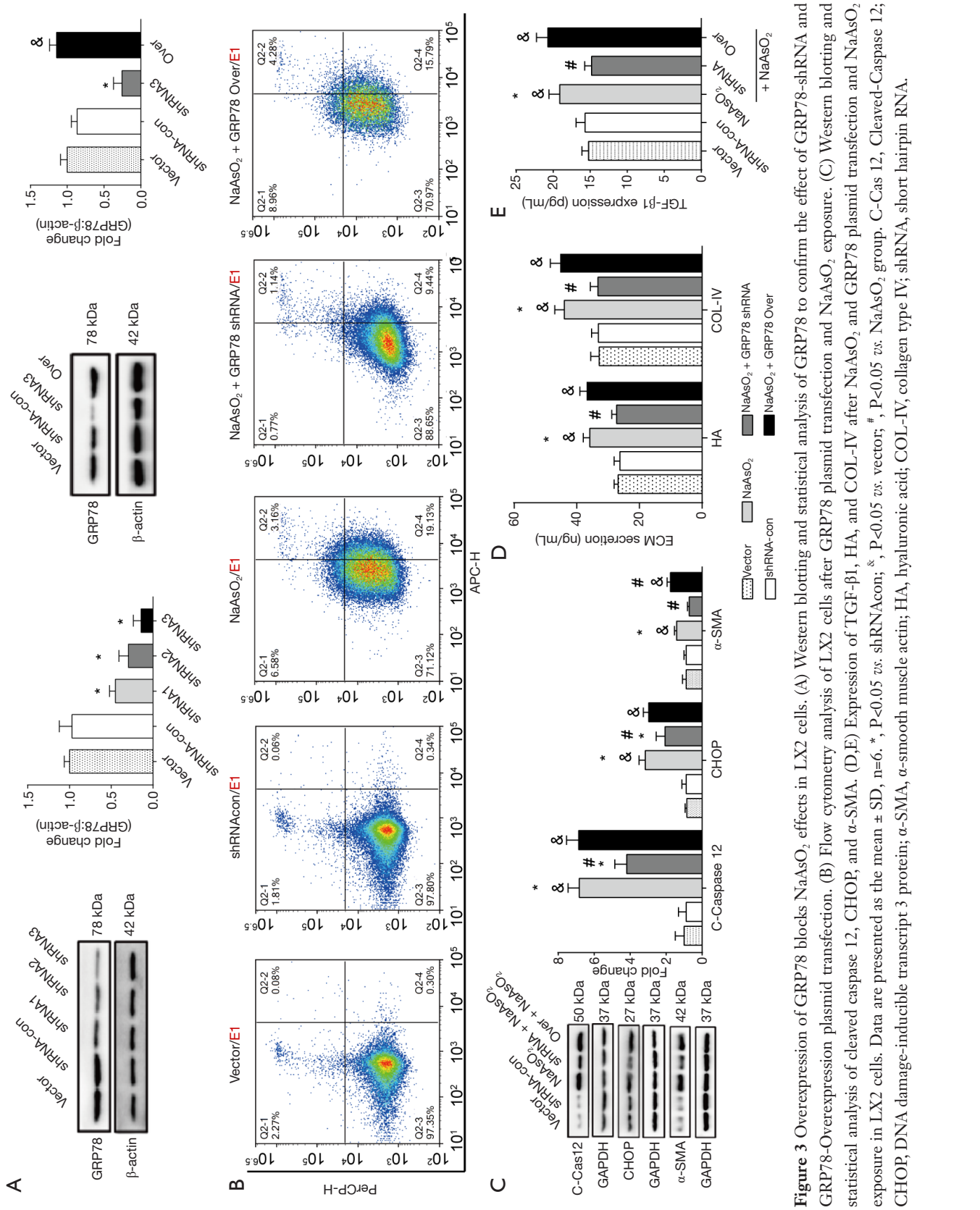

Figure 3 Overexpression of GRP78 blocks $NaAsO_2$ effects in LX2 cells. (A) Western blotting and statistical analysis of GRP78 to confirm the effect of GRP78-shRNA and GRP78-Overexpression plasmid transfection. (B) Flow cytometry analysis of LX2 cells after GRP78 plasmid transfection and $NaAsO_2$ exposure. (C) Western blotting and statistical analysis of cleaved caspase 12, CHOP, and α-SMA. (D,E) Expression of TGF-β1, HA, and COL-IV after $NaAsO_2$ and GRP78 plasmid transfection and $NaAsO_2$ exposure in LX2 cells. Data are presented as the mean ± SD, n=6. *, $P<0.05$ *vs.* shRNAcon; &, $P<0.05$ *vs.* vector; #, $P<0.05$ *vs.* $NaAsO_2$ group. C-Cas 12, Cleaved-Caspase 12; CHOP, DNA damage-inducible transcript 3 protein; α-SMA, α-smooth muscle actin; HA, hyaluronic acid; COL-IV, collagen type IV; shRNA, short hairpin RNA.

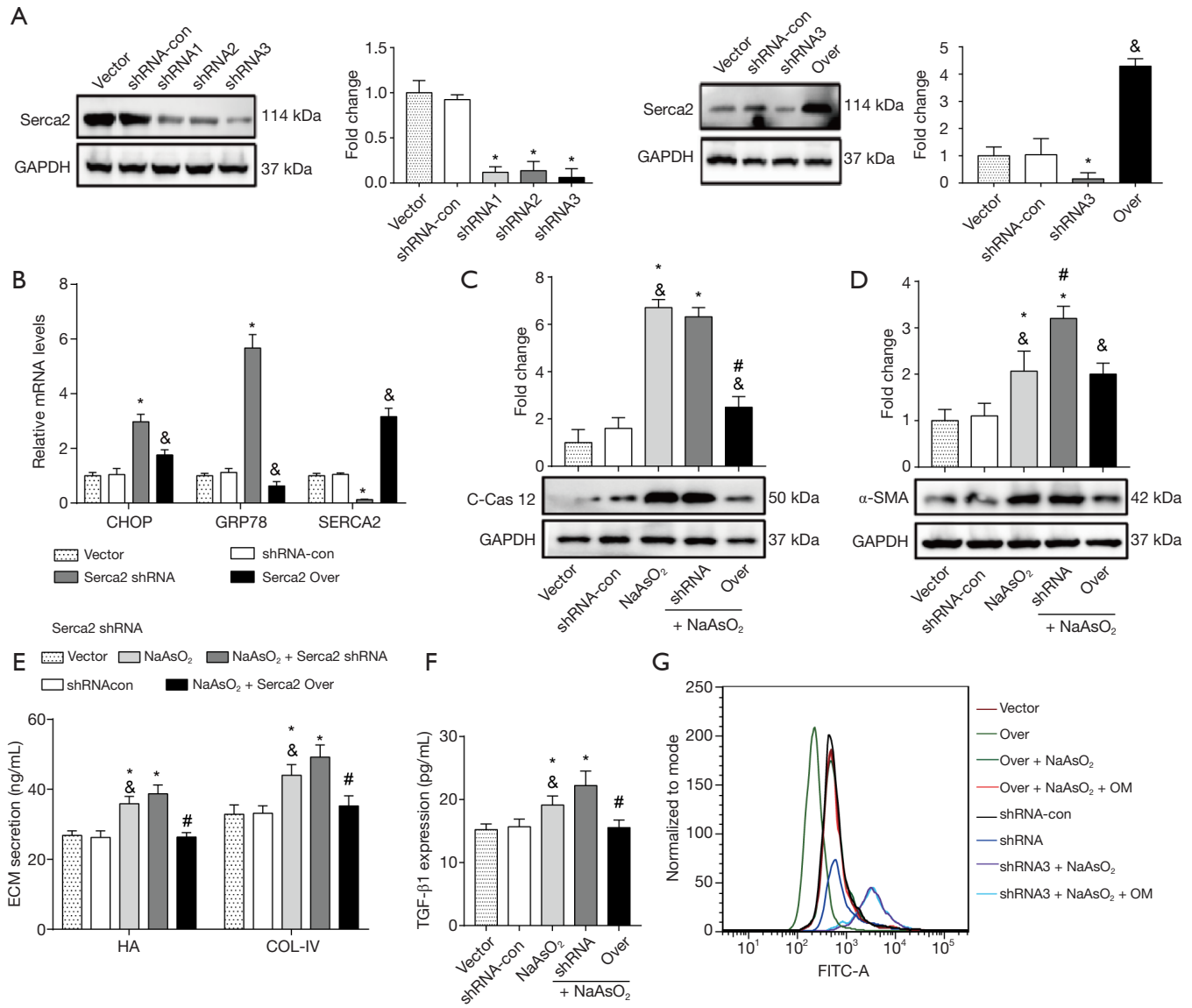

Figure 4 SERCA2 knockdown blocks $NaAsO_2$-induced effects in LX2 cells. (A) Western blotting and statistical analysis of SERCA2 to confirm the effect of SERCA2-shRNA and SERCA2-Overexpression plasmid transfection. (B) The relative mRNA of CHOP, GRP78, SERCA2 after shRNA, and Overexpression plasmid transfection. (C,D) Western blotting and statistical analysis of C-caspase12 and α-SMA. (E,F) Expression of TGF-β1, HA, and COL-IV after $NaAsO_2$ and SERCA2 plasmid transfection in LX2 cells. (G) Intracellular calcium concentration after SERCA2 knockdown and overexpression, $NaAsO_2$, and OM treatment. Data are presented as the mean ± SD, n=6. *, P<0.05 *vs.* shRNAcon; $^{\&}$, P<0.05 *vs.* vector; $^{\#}$, P<0.05 *vs.* $NaAsO_2$ group. C-Cas 12, Cleaved-Caspase 12; CHOP, DNA damage-inducible transcript 3 protein; shRNA, short hairpin RNA; α-SMA, α-smooth muscle actin; HA, hyaluronic acid; COL-IV, collagen type IV; OM, oxymatrine.

Discussion

Arsenic, a group 1 carcinogen, can affect many organs, including the kidneys, skin, and liver. As the main target of arsenic toxicity, chronic arsenic exposure induces severe liver fibrosis, and several types of cancer (7-9). It is presumed that HF is a reversible study to find effective treatments to alleviate HF are ongoing. Earlier studies have reported that most of the ECMs are produced by activated HSCs (20,21). HSC cells are rich in ER, which is more sensitive to changes in calcium

homeostasis and various external stimuli. The ER is one of the most important organelles in the cell, as well as an important store of calcium ions. It is a modification site for synthesized proteins. It has functions such as regulating the folding and aggregation of intracellular proteins after synthesis, cell stress response, and maintaining intracellular Ca^{2+} levels. When cells are continuously stimulated, unfolded and misfolded proteins accumulate in the ER, and the homeostasis of calcium ions in the ER is dysregulated, different degrees of ERS will occur in the ER. As a marker protein of ER stress, GRP78 normally binds to three sensing proteins on the ER membrane: protein kinase-like endoplasmic reticulum kinase (PERK), inositol-demanding enzyme 1 (IRE-1), transcription activator 6 (ATF6) receptors and is inactivated. When cells are overstimulated and Ca^{2+} homeostasis is unbalanced, GRP78 dissociates from the receptor, causing the occurrence of ER stress, initiating downstream signaling pathways: phosphorylation of PERK, IRE-1 and ATF6 activation downstream signaling pathways such as PAK-2, MAPK, ERK1/2 and NF-kB to regulate cell differentiation and proliferation, and exert cell defense functions. On the other hand, phosphorylation of eIF2alpha by activated PERK activates the expression of DNA damage-inducing family gene 153 (CHOP), which acts as a transcription factor in the ER stress pathway to induce apoptosis. Activation of ATF6 can increase the expression of GRP78 and CHOP. IRE-1 activates XBP1, leading to the transcription of chaperones, thus contributing to the reduction of protein loading into the ER. Caspase12 is a specific aspartate protease in ER stress and one of the marker proteins of ER stress generation. And HSC activation and ECM secretion may be the significant drivers of HF (5,10,21). In the present study, it was found $NaAsO_2$ treated LX2 cells secreted ECM, which was alleviated by treatment with oxymatrine, suggesting that LX2 can be used as an *in vitro* model for HF. In the earlier studies, they investigated the ER stress in the HF model (9,11). And they believed that the unfolded protein response (UPR) plays a crucial role in HF progression (11).

The present study indicated that ER stress and calcium homeostasis play essential roles in the progression of HSC activation and ECM secretion, which are the major causes of HF. Also, the oxymatrine attenuates the $NaAsO_2$-induced HSC activation and ECM secretion through the ER stress and calcium homeostasis, which might be the mechanism of oxymatrine produced anti-fibrotic. Moreover, attenuation of ER stress by knocking down GRP78 could also produce a similar effect. In the present study, we also found that cellular calcium levels were affected by $NaAsO_2$ exposure and restored by oxymatrine treatment. $NaAsO_2$ affected SERCA2 expression to disrupt intracellular calcium homeostasis, causing ER stress, while oxymatrine blocked these effects through the same mechanisms. And overexpression of SERCA2 to restore the cellular calcium rescued $NaAsO_2$-induced ECM secretion and LX2 apoptosis. Therefore, it was concluded that regulation of cellular calcium homeostasis and ER stress is essential for HSC activation and ECM secretion. It suggests that ER stress and calcium homeostasis might be the major causes of HF and anti-fibrotic effects.

In conclusion, $NaAsO_2$ exposure disrupted calcium homeostasis to produce ER stress, leading to HSC activation and ECM secretion. Oxymatrine restores calcium homeostasis to attenuate ER stress and alleviate them. The present study suggests that ER and calcium homeostasis might be worthwhile targets to prevent and treat HF. Further, studies aiming to develop new drugs for HF should focus on ER stress and cellular calcium homeostasis. The present study tested the roles of ER stress and calcium following $NaAsO_2$ exposure and oxymatrine treatment; however, further studies are required to verify whether this is the general mechanism for HF and the anti-fibrotic effects of oxymatrine. ER's stress and calcium homeostasis were investigated in the LX2 cell model; however, studies using animal models and clinical samples are still needed.

Acknowledgments

Funding: The present study was supported by the National Natural Science Foundation of China (No.81460484).

Footnote

Reporting Checklist: The authors have completed the MDAR reporting checklist. Available at http://dx.doi.org/10.21037/atm-20-5881

Data Sharing Statement: Available at http://dx.doi.org/10.21037/atm-20-5881

Conflicts of Interest: All authors have completed the ICMJE uniform disclosure form (available at http://dx.doi.org/10.21037/atm-20-5881). The authors have no conflicts of interest to declare.

Ethical Statement: The authors are accountable for all aspects of the work in ensuring that questions related to the accuracy or integrity of any part of the work are appropriately investigated and resolved.

References

1. Popov Y, Schuppan D. Targeting liver fibrosis: strategies for development and validation of antifibrotic therapies. Hepatology 2009;50:1294-306.
2. Krenkel O, Puengel T, Govaere O, et al. Therapeutic inhibition of inflammatory monocyte recruitment reduces steatohepatitis and liver fibrosis. Hepatology 2018;67:1270-83.
3. Lai JC, Verna EC, Brown RS Jr, et al. Hepatitis C virus-infected women have a higher risk of advanced fibrosis and graft loss after liver transplantation than men. Hepatology 2011;54:418-24.
4. Ligat G, Schuster C, Baumert TF. Hepatitis B Virus Core Variants, Liver Fibrosis, and Hepatocellular Carcinoma. Hepatology 2019;69:5-8.
5. Kostallari E, Hirsova P, Prasnicka A, et al. Hepatic stellate cell-derived platelet-derived growth factor receptor-alpha-enriched extracellular vesicles promote liver fibrosis in mice through SHP2. Hepatology 2018;68:333-48.
6. Karagas MR, Gossai A, Pierce B, et al. Drinking Water Arsenic Contamination, Skin Lesions, and Malignancies: A Systematic Review of the Global Evidence. Curr Environ Health Rep 2015;2:52-68.
7. Liu J, Waalkes MP. Liver is a target of arsenic carcinogenesis. Toxicol Sci 2008;105:24-32.
8. Pan X, Dai Y, Li X, et al. Inhibition of arsenic-induced rat liver injury by grape seed exact through suppression of NADPH oxidase and TGF-β/Smad activation. Toxicol Appl Pharmacol 2011;254:323-31.
9. Yang M, Wang C, Li S, et al. Annexin A2 promotes liver fibrosis by mediating von Willebrand factor secretion. Dig Liver Dis 2017;49:780-8.
10. Du M, Zhang J, Xu D, et al. Inhibition of pro collagen I expression by oxymatrine in hepatic stellate cells is mediated via nuclear translocation of Y box binding protein 1. Mol Med Rep 2015;12:8101-6.
11. Dong S, Cai FF, Chen QL, et al. Chinese herbal formula Fuzheng Huayu alleviates CCl4-induced liver fibrosis in rats: a transcriptomic and proteomic analysis. Acta Pharmacol Sin 2018;39:930-41.
12. Mao YM, Zeng MD, Lu LG, et al. Capsule oxymatrine in treatment of hepatic fibrosis due to chronic viral hepatitis: a randomized, double blind, placebo-controlled, multicenter clinical study. World J Gastroenterol 2004;10:3269-73.
13. Jiang X, Xie L, Huang C, et al. Oral oxymatrine for hepatitis B cirrhosis: A systematic review protocol. Medicine (Baltimore) 2018;97:e13482.
14. Shi GF, Li Q. Effects of oxymatrine on experimental hepatic fibrosis and its mechanism in vivo. World J Gastroenterol 2005;11:268-71.
15. Chai NL, Fu Q, Shi H, et al. Oxymatrine liposome attenuates hepatic fibrosis via targeting hepatic stellate cells. World J Gastroenterol 2012;18:4199-206.
16. Wu XL, Zeng WZ, Jiang MD, et al. Effect of Oxymatrine on the TGFbeta-Smad signaling pathway in rats with CCl4-induced hepatic fibrosis. World J Gastroenterol 2008;14:2100-5.
17. Pan XY, Yang Y, Meng HW, et al. DNA Methylation of PTGIS Enhances Hepatic Stellate Cells Activation and Liver Fibrogenesis. Front Pharmacol 2018;9:553.
18. Hennig H, Rees P, Blasi T, et al. An open-source solution for advanced imaging flow cytometry data analysis using machine learning. Methods 2017;112:201-10.
19. Lee WK, Dittmar T. Cytosolic calcium measurements in renal epithelial cells by flow cytometry. J Vis Exp 2014:e51857.
20. Huang Y, Li X, Wang Y, et al. Endoplasmic reticulum stress-induced hepatic stellate cell apoptosis through calcium-mediated JNK/P38 MAPK and Calpain/Caspase-12 pathways. Mol Cell Biochem 2014;394:1-12.
21. Prestigiacomo V, Weston A, Messner S, Lampart F, Suter-Dick L. Pro-fibrotic compounds induce stellate cell activation, ECM-remodelling and Nrf2 activation in a human 3D-multicellular model of liver fibrosis. PloS One 2017;12:e0179995.

(English Language Editor: J. Chapnick)

Cite this article as: Wang H, Han B, Wang N, Lu Y, Gao T, Qu Z, Yang H, Yang Q. Oxymatrine attenuates arsenic-induced endoplasmic reticulum stress and calcium dyshomeostasis in hepatic stellate cells. Ann Transl Med 2020;8(18):1171. doi: 10.21037/atm-20-5881

